

pubs.acs.org/JACS Article

Origins of Catalyst-Controlled Selectivity in Ag-Catalyzed Regiodivergent C—H Amination

Yue Fu, Emily E. Zerull, Jennifer M. Schomaker,* and Peng Liu*



Cite This: J. Am. Chem. Soc. 2022, 144, 2735-2746



ACCESS I

Metrics & More

Article Recommendations

s Supporting Information

ABSTRACT: Ag-catalyzed nitrene transfer (NT) converts C–H bonds into valuable C–N bonds. These reactions offer a promising strategy for catalyst-controlled regiodivergent functionalization of different types of reactive C–H bonds, as the regioselectivity is tunable by varying the steric and electronic environments around the Ag nitrene, as well as the identity of the nitrene precursors and the tether length. Therefore, a unified understanding of how these individual factors affect the regioselectivity is key to the rational design of highly selective and regiodivergent C–H amination reactions. Herein, we report a computational study of various Agcatalyzed NT reactions that indicates a concerted H-atom transfer (HAT)/C–N bond formation mechanism. A detailed analysis was

carried out on the effects of the C–H bond dissociation enthalpy (BDE), charge transfer, ligand–substrate steric repulsions, and transition state ring strain on the stability of the C–H insertion transition states with different Ag nitrene complexes. The ancillary ligands on the Ag and the nitrene precursor identity both affect transition state geometries to furnish differing sensitivities to the BDE, tether length, and electronic effects of the reactive C–H bonds. Based on our understanding of the dominant factors that control selectivity, we established a rational catalyst and precursor selection approach for regiodivergent amination of diverse C–H bonds. The computationally predicted regiodivergent amination of β - and γ -C–H bonds of aliphatic alcohol derivatives was validated by experimental studies.

INTRODUCTION

The efficient construction of new C-N bonds from C-H bonds is of great interest due to the prevalence of amines in pharmaceuticals, agrochemicals, and bioactive natural products. Many different transition metal catalysts are capable of C-H bond amination; however, there is an ongoing challenge to identify strategies for tunable catalyst-controlled selectivity in reactions with multiple potential reactive sites. In this context, recently, the development of Ag-catalyzed nitrene transfer (NT) (Figure 1a) has attracted attention. The diversity of ligands able to support Ag catalysts results in a broad range of steric and electronic environments around the reactive center, offering unique opportunities to achieve catalyst-controlled regio- and enantioselectivities.

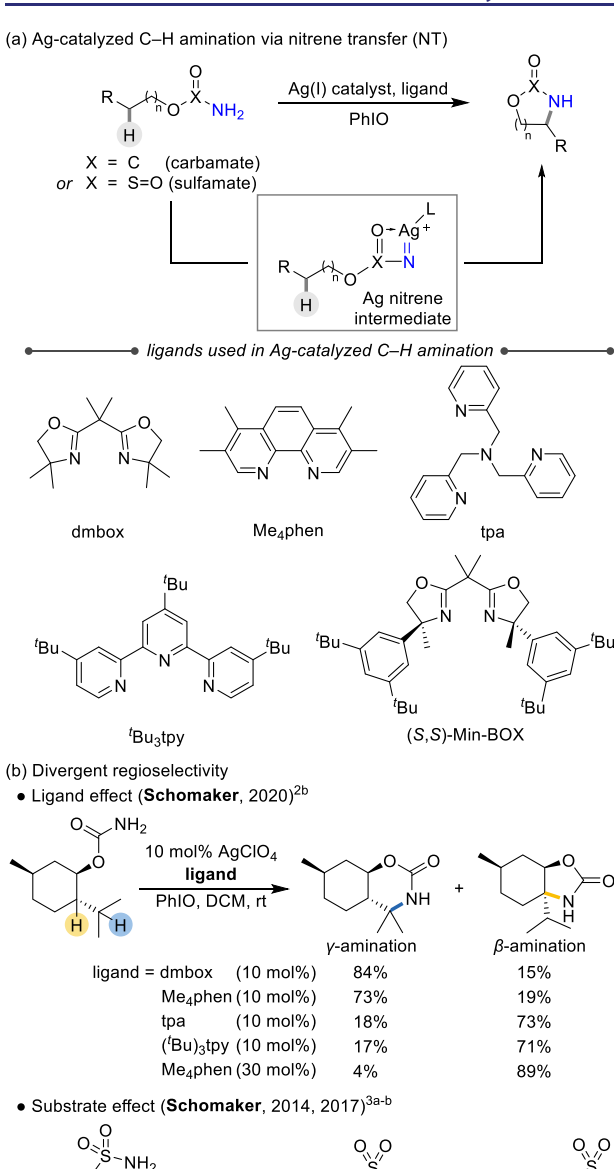
Schomaker et al. have demonstrated that the expected regioselectivity of Ag-catalyzed C–H amination can be modulated, and sometimes completely reversed, by the electronic and steric properties of the substrate, as well as the identity of the ancillary ligands on the metal (Figure 1b).² In addition, reactions using precursors with different nitrogen protecting groups (e.g., carbamate and sulfamate) may yield complete reversal in regioselectivities. These reactions provide access to both 1,2- and 1,3-diffunctionalized amine products after removal of the *N*-protecting group. Despite these interesting observations, the origin of the catalyst and substrate

effects on regioselectivity is still not well understood. The regioselectivity appears to be controlled by the combination of several factors, including bond dissociation enthalpy (BDE), electronic properties and the steric environment of the C-H bonds, tether length, the ancillary ligands on Ag, and the identity of the precursors. 2b,3 We surmised that a holistic understanding of the interplay of these different factors would offer practical guidance to broaden the scope of the regioselective amination, develop Ag catalysts to effectively distinguish between C-H bonds with similar BDEs and steric environments, and override inherent substrate preference to favor less reactive sites. Herein, we report a computational study to understand the reaction mechanism of the Agcatalyzed amination and gain insights into the origin of reactivity and regioselectivity. We analyze why different catalyst systems favor different types of C-H bonds through the lens of their differing sensitivities to BDEs, tether length,

Received: November 16, 2021 Published: February 7, 2022







AgClO₄, tpa PhIO, DCM, rt benzylic 3° aliphatic BDE ≈ 86 BDE ≈ 93 Ar = 4-OMe-Ph, R =Me 15% 70% Ar = Ph, R =Me 60% 25% $Ar = 4-CF_3-Ph, R = Me$ 42% 54%

63%

0%

(c) This work: mechanistically-driven approach for regioselectivity prediction

Ar = Ph, R = Pr

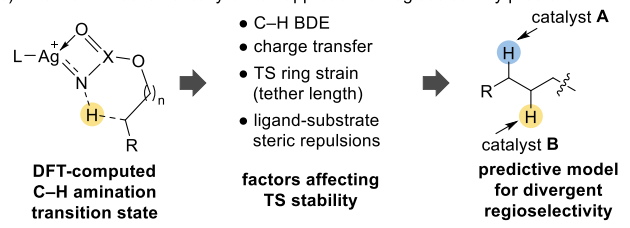


Figure 1. Tunable regioselectivities in the Ag-catalyzed C-H amination. BDEs are in kcal/mol.

electronic effects, and ligand-substrate steric repulsions (Figure 1c). We establish an approach to rationally select the most effective Ag catalyst and precursor group for a desired regioselective amination based on the intrinsic electronic and steric properties of the C–H bonds. Experimental studies were performed to validate the computationally predicted regioselectivity trends in different catalyst systems. This mechanistically guided approach was applied to achieve catalystcontrolled regiodivergent amination of alkyl C-H bonds that display similar steric and electronic environments.

COMPUTATIONAL METHODS

Density functional theory (DFT) calculations, including geometry optimization and single-point energy calculations, were performed with the Gaussian 16 software package. 4 Geometries were optimized in the gas phase using the $\omega B97X-D^5$ functional and a mixed basis set of def2-TZVPP for Ag and def2-SVP for other atoms. Single-point energies were calculated using ω B97X-D and the def2-TZVPP basis set for all atoms in dichloromethane (DCM) using the SMD solvation model.⁶ Conformers of each ground state and transition state structure were studied by manual conformational search and automated conformational sampling using CREST and GFN2xTB. Low-energy conformers from the CREST/xTB conformational sampling were then re-optimized using DFT at the aforementioned level of theory. The reported Gibbs free energies and enthalpies in solution include thermal corrections computed at 298 K at the standard concentration (1 mol/L) using GoodVibes. 9 BDE and transition state ring strain energy (ΔH_s) were also calculated at the ωB97X-D/def2-TZVPP, SMD(DCM)//ωB97X-D/def2-SVP-def2-TZVPP(Ag) level of theory. PNO-LCCSD(T)-F12 benchmark calculations were performed using Molpro 2020.2. CASPT2 benchmark calculations were performed using OpenMolcas. 13 Details of the PNO-LCCSD(T)-F12 and CASPT2 calculations are provided in the Supporting Information. Among the tested DFT methods, ωB97X-D provided the best agreement for the activation energy of C–H amination of carbamate 1 compared with the PNO-LCCSD-(T)-F12 and CASPT2 results. 14 ω B97X-D also provided the best agreement with the experimental regioselectivity of a series of intramolecular competition reactions (see Figures S1-S3). Therefore, we used ωB97X-D for geometry optimizations and single-point energy calculations in the present study.

RESULTS AND DISCUSSION

Reaction Mechanisms of the Ag-Catalyzed C-H **Amination via NT.** The proposed mechanism (Figure 2) of

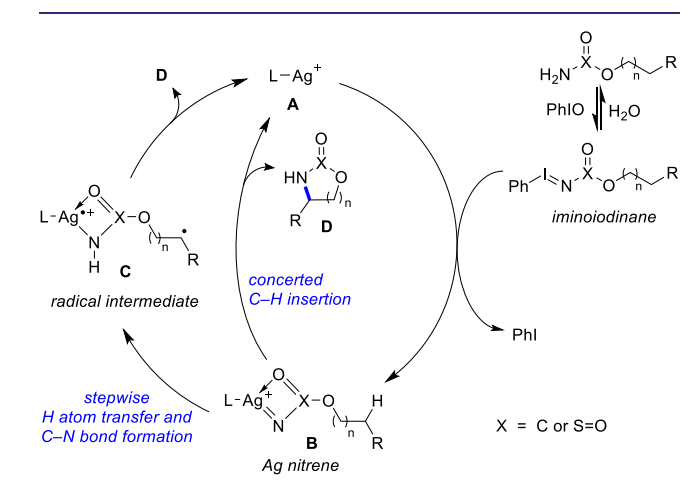


Figure 2. Proposed mechanisms of the Ag-catalyzed C-H amination.

the Ag-catalyzed C-H amination involves formation of Ag nitrene species B from Ag(I) precatalyst A and an iminoiodinane formed by the condensation of the carbamate or sulfamate substrate with PhIO. The subsequent C-H insertion with the Ag nitrene may involve two possible mechanisms: (a) H-atom transfer to the Ag nitrene to form an

alkyl radical intermediate C, followed by radical recombination to form the C–N bond in the final product D; and (b) a concerted C–H insertion process where the alkyl radical is not involved. L2,15 Experimental mechanistic studies, including radical clock and stereospecificity experiments, appear to support a concerted mechanism without long-lived radical intermediates in both the (tpa)Ag(OTf)-catalyzed intramolecular amination of sulfamates and the (dmbox)Ag(ClO₄)-catalyzed amination of carbamates. However, the previous studies could not rule out the possibility of a stepwise pathway involving short-lived radical intermediates and rapid radical rebound to form the new C–N bond.

To investigate the most favorable amination mechanism, we first calculated the reaction energy profile of the (dmbox)Ag-(ClO₄)-catalyzed benzylic C–H amination of carbamate 1 at the ω B97X-D/def2-TZVPP, SMD(DCM)// ω B97X-D/def2-SVP-def2-TZVPP(Ag) level of theory (Figure 3). The

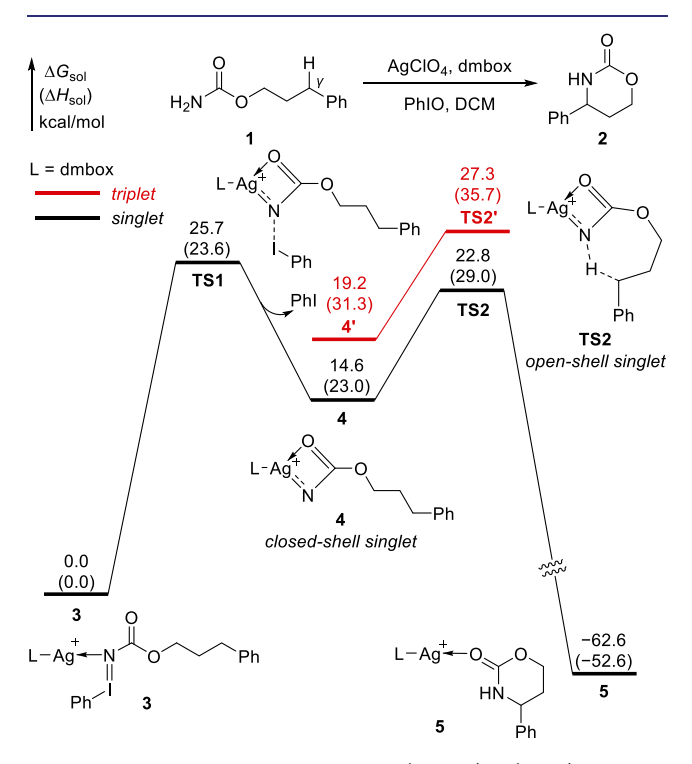


Figure 3. Reaction energy profile of the $(dmbox)Ag(ClO_4)$ -catalyzed C-H bond amination of carbamate 1.

reaction is initiated via condensation of substrate 1 with PhIO to form an iminoiodinane, which coordinates to the Ag(I) precatalyst to form the dative complex 3. The nitrene formation via PhI dissociation (TS1) requires an activation free energy of 25.7 kcal/mol. The resulting Ag nitrene 4 is a closed-shell singlet and is 14.6 kcal/mol less stable than 3. The singlet Ag nitrene (4) favors a four-coordinate square planar geometry with strong coordination of the carbonyl oxygen to the Ag center. 16 The most favorable C-H amination pathway involves C-H insertion via an open-shell singlet transition state TS2 with a relatively low barrier of 8.2 kcal/mol with respect to 4. Intrinsic reaction coordinate calculations indicate that the C-H insertion (TS2) is a concerted process (see Figure S24); after the H-atom transfer, the C-N bond is formed spontaneously to furnish the amination product complex 5, while the open-shell character rapidly diminishes. Because **TS2** is lower in energy than **TS1**, the rate-determining step of the catalytic cycle is the nitrene formation via **TS1**. The endergonicity of nitrene formation and the high reactivity of the Ag nitrene complex in C–H insertion is consistent with the challenges associated with the isolation and characterization of Ag nitrene intermediates. ¹⁸

Because previous computational studies indicated that both singlet and triplet Ag nitrene complexes may be involved in the C-H amination and alkene aziridination reactions, 19 we studied the spin states of the Ag nitrene intermediate and the C-H insertion transition state using different levels of theory, including several DFT methods, explicitly correlated local coupled cluster [PNO-LCCSD(T)-F12] and complete active-space second-order perturbation theory (CASPT2) calculations (Figure S1). These calculations predicted that the singlet Ag nitrene (4) and the C-H insertion transition state (TS2) are more stable than the corresponding triplet structures. At the ω B97x-D level of theory, the triplet C-H insertion transition state (TS2') is 4.5 kcal/mol higher in energy than the open-shell singlet transition state (TS2) in the (dmbox)Ag(ClO₄)-catalyzed amination of carbamate 1. The energy difference between singlet and triplet C-H insertion pathways is affected by the ancillary ligand on the Ag, as well as the identity of the nitrene precursor (see Tables S1-S4 and Figures S5-S23). Nonetheless, our PNO-LCCSD(T)-F12 and CASPT2 calculations suggest that the singlet C-H insertion pathway is more favorable for four types of Ag nitrenes supported by dmbox and tpa ligands and derived from carbamate and sulfamate precursors. Therefore, only singlet C–H insertion pathways are considered in the present study.

Catalyst-Controlled Regiodivergent C-H Amination of n-Butyl Carbamate—A Case Study. After establishing the favored mechanism of the Ag-catalyzed intramolecular C-H amination, we chose the Ag-catalyzed C-H amination of nbutyl carbamate 6 as a model reaction to identify factors affecting the regioselectivity. This carbamate substrate was chosen because tunable regioselectivity has been achieved experimentally for carbamate starting materials with sterically and electronically unbiased β - and γ -C-H bonds. For example, amination of a menthol-derived carbamate yielded γ-product selectively with a dmbox-supported Ag catalyst, while the regioselectivity is completely reversed to yield β -selectivity with tpa- and ^tBu₃tpy-supported Ag catalysts (Figure 1b). ^{2b} Although experimental studies of 6 have not been reported, we surmised that due to the similar steric and electronic environment of its β - and γ -C-H bonds, catalyst-controlled divergent regioselectivity may be achieved. Indeed, our DFT calculations predict that the reaction is selective for γ -C-H amination ($\Delta \Delta G^{\ddagger} = 1.5 \text{ kcal/mol}$) when a dmbox ligand is used, while the same reaction favors the β -C-H amination product $(\Delta \Delta G^{\ddagger} = -1.0 \text{ kcal/mol})$ when a tpa ligand is used instead. This computationally predicted regioselectivity trend is consistent with the catalyst-controlled selectivity in aminations of other carbamate substrates (e.g., Figure 1b^{2b}); it was later validated experimentally (vide infra). Careful analysis of the C-H insertion transition states (TS3, TS4) revealed that the main reason for the catalyst-controlled divergent regioselectivity is the different steric properties of the bidentate dmbox ligand compared to the more crowded multidentate tpa ligand. In the dmbox-supported C-H insertion transition states (TS3- γ and TS3- β), ligandsubstrate steric repulsions are not observed. The preference for γ -C-H amination can be attributed to the slightly weaker γ -C-H bond compared to the β -C-H bond (BDE = 96.8 and

98.0 kcal/mol, respectively) or the difference between ring strain energies of the six- and seven-membered cyclic transition states (a detailed discussion about ring strain effects is given below). In contrast, when the more crowded tpa ligand is used, the γ -C-H insertion transition state (TS4- γ) suffers from greater ligand-substrate steric repulsions as compared to the β -C-H insertion transition state (TS4- β). TS4- γ is destabilized by steric repulsion between the carbamate carbonyl oxygen and one of the pyridine arms on the tpa ligand (d(O···H) = 2.39 Å). The ligand-substrate steric repulsion is diminished in TS4- β , where the carbamate carbonyl is placed further away from the ligand due to the sterically less demanding six-membered ring as compared to the seven-membered ring in TS4- γ .

Although the ligand steric effects nicely explain the origin of divergent regioselectivity in the amination of 6, a more general regioselectivity model is still needed to understand the regioselectivity control with other substrates and ancillary ligands. This is due to several other factors that may also affect the transition state stability and thus the regioselectivity. These factors include substrate properties, such as the BDE and electronic properties of the C-H bond being activated, as well as the electronic effects of the ancillary ligand on the Ag nitrene. In particular, the donor ability of the ancillary ligand affects the amount of electron transfer from the C-H bond to the Ag nitrene and the early/lateness of the C-H insertion transition state. For example, transition states TS4- γ and TS4- β with the more electron-rich tpa ligand involve less electron transfer from the C-H bond and shorter bond distances of the cleaving C-H bond than transition states with dmbox (TS3-y and $TS3-\beta$) (Figure 4). Therefore, reactions with these different ligands may have different sensitivities to substrate properties, such as BDE and electronic effects.

Another question that needs to be carefully evaluated is why the identity of the nitrene precursor has such a dramatic impact on the regioselectivity. While there are several examples of regiodivergent amination of either β - or γ -C-H bonds in carbamate precursors, reactions with sulfamates are often highly γ -selective, regardless of the ligand used. Changing the nitrene precursor from carbamate to sulfamate may affect the ring strain energy difference between the seven- and sixmembered cyclic transition states, 20 the catalyst-substrate noncovalent interactions (Figures S25 and S26),3b or the strength of the coordination of the carbonyl and sulfonyl groups to the Ag center. These multifaceted interactions between the Ag nitrene and the C-H bond pose a significant challenge in rationally predicting the regioselectivity of the amination. On the other hand, they also offer promising opportunities to achieve catalyst-controlled regioselectivity by fine-tuning the electronic and steric properties of the Ag nitrene. These initial computational analyses prompted us to perform a detailed investigation on how these individual factors affect the reactivity of the C-H insertion with different Ag nitrene complexes.

Effects of BDE on Reactivity. We computed the C-H insertion activation free energies of four different types of Ag nitrene species (Types I-IV) undergoing reaction with C-H bonds in substrates with various BDE values (Figure 5a). These four types of Ag nitrenes were chosen because they include ancillary ligands with different denticities (dmbox, bidentate and tpa, tetradentate) and precursors with planar (carbamate) and tetrahedral-shaped (sulfamate) groups attached to the nitrenes. We surmised that these factors may

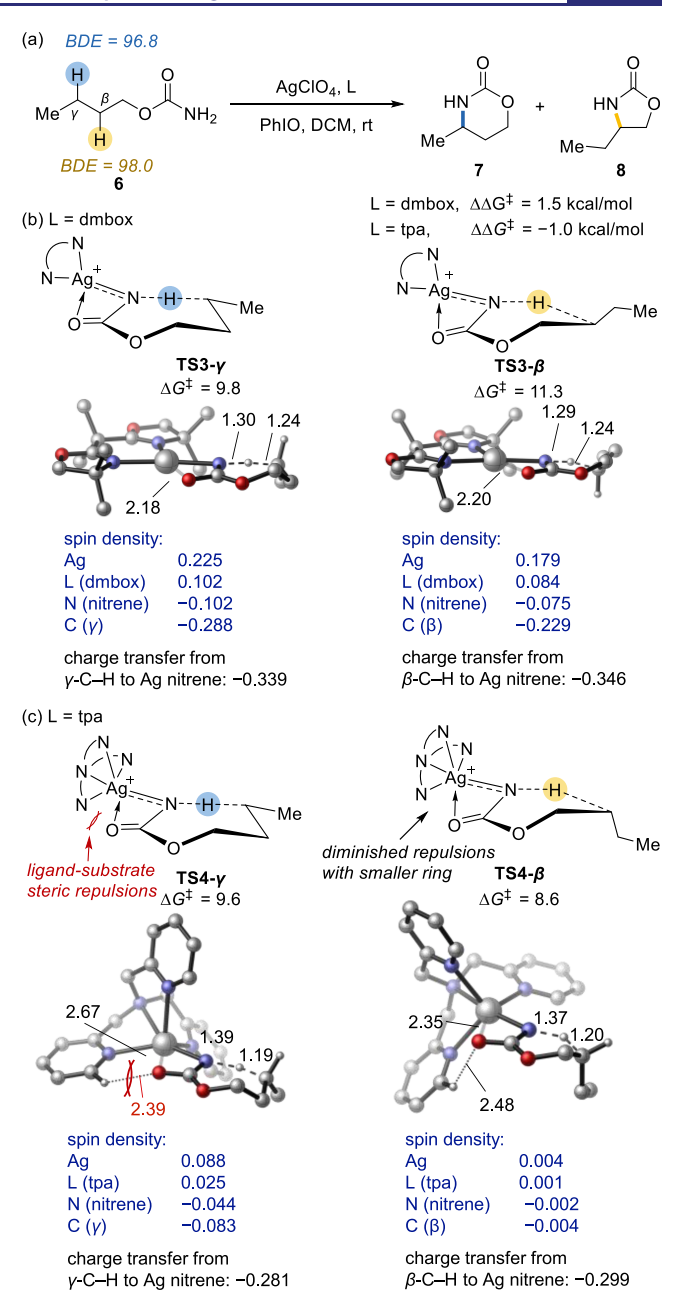
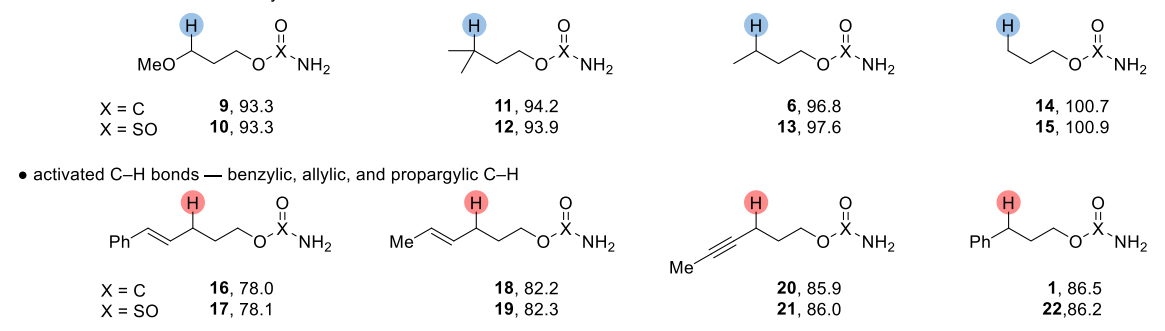


Figure 4. Ligand effect on regioselectivities in the Ag-catalyzed C–H amination of carbamate **6.** BDEs are in kcal/mol. ΔG^{\ddagger} in this and subsequent figures are in kcal/mol with respect to the corresponding Ag nitrene intermediates.

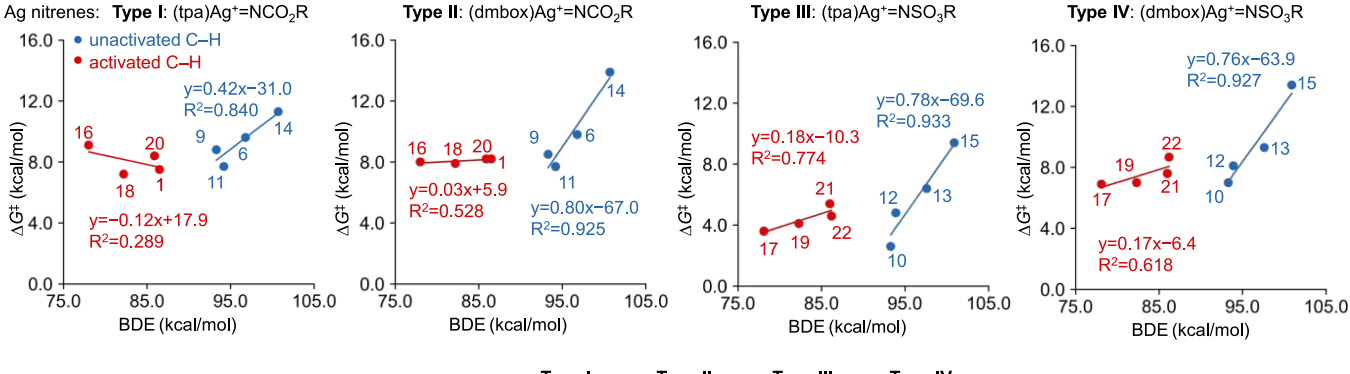
impact the transition state geometry and ligand—substrate interactions. Here, only γ -C–H bonds are included to study BDE effects and avoid the potential impacts of the tether length (the effects of the tether length will be discussed later). BDE values are often recognized as the primary factor affecting the reactivity of C–H bonds in hydrogen atom abstraction reactions, 21 including NT. 22 However, the computed activation free energies do not show good overall correlations with C–H BDE in any of the four types of Ag nitrenes studied (Figure Sb). Instead, bimodal relationships were observed. The reactivity of alkyl and ether α -C–H bonds (named "unactivated" C–H, 6, 9–15) correlates well with their BDEs with moderate-to-large slopes (0.42~0.80). In contrast, the reactivity of C–H bonds adjacent to a sp² or sp carbon

(a) C-H bond BDEs (in kcal/mol) in carbamate (X = C) and sulfamate (X = S=O) precursors

• unactivated C–H bonds — alkyl C–H and ether α-C–H



(b) Effects of BDE on C-H insertion reactivity with different types of Ag nitrene complexes



	Type I	Type II	Type III	Type IV
ligand	tpa	dmbox	tpa	dmbox
precursor	carbamate	carbamate	sulfamate	sulfamate
sensitivity to BDE of unactivated C–H bonds [†]	0.42	0.80	0.78	0.76
sensitivity to BDE of activated C–H bonds [†]	-0.12	0.03	0.18	0.17

 $^{^\}dagger$ Sensitivity is derived from the slope of the correlation between ΔG^\ddagger and C–H BDE.

Figure 5. Effects of C—H BDE on the activation free energies of C—H insertion with different Ag nitrene complexes derived from carbamate and sulfamate precursors.

center, such as allylic, propargylic, and benzylic C-H bonds (named "activated" C-H, 1, 16-22), are much less sensitive to BDE (slope = $-0.12 \sim 0.18$). Although similar bimodal correlations have been observed in C–H oxidations using DMDO and $\text{CumO} \bullet$, ^{23,24} the extremely low sensitivity of activated C-H bonds to BDE is a unique feature of the Agcatalyzed amination, as transition metal-catalyzed C-H hydroxylation reactions involving metal oxo species are generally more sensitive to BDE.²³ For example, the slopes of the DMDO- and CumOo-mediated HAT with activated C-H bonds are 0.35 and 0.23, respectively, much larger than those in the Ag-catalyzed amination. The lower sensitivity to BDE in reactions of activated C-H bonds with Ag nitrenes can be explained by the Hammond postulate—the highly exergonic reactions have more reactant-like transition states, in which the stability of the alkyl radical plays a less prominent role in the reaction barriers. It should be noted that the carbamate-derived Ag nitrenes (Figure 5b, Types I and II) are completely insensitive to the BDE in reactions with activated C-H bonds. The lack of a strong influence of BDE suggests that the regioselectivity of the Ag-catalyzed amination of these activated C-H bonds is modulated by other factors, such as ligand-substrate steric repulsions or dispersion interactions, to override the intrinsic preference for reaction based on simple bond strengths.

In reactions with unactivated C-H bonds, the reactivity is more sensitive to C-H BDEs, as these reactions are less exergonic and generally have later transition state structures with longer C-H bond distances (Table S5). Another interesting trend revealed by Figure 5 is that the reactions with tpa-supported Ag nitrenes derived from carbamate precursors (Type I) are the least sensitive to C-H BDE in reactions with unactivated C-H bonds. In these reactions, a moderate slope of 0.42 was obtained, compared to the slopes of ~0.8 in the reactions of unactivated C-H bonds with the other three types of Ag nitrenes (Types II-IV). These results suggest that the Ag(tpa)-catalyzed reactions with carbamates are less sensitive to the strength of unactivated C-H bonds. Thus, this catalyst system offers the best chance to override the BDE effect to selectively activate a stronger unactivated C-H bond and promote reactivity of primary C-H bond amination by fine-tuning other factors controlling the TS stability.

Effects of Tether Length on Reactivity and Selectivity. Next, we investigated the effects of tether length, that is, whether the C–H bond is located at the β - or γ -position of the carbamate or sulfamate precursor, on the regioselectivity of C–H insertion. Although the computed regioselectivity of the amination of n-butyl carbamate **6** is strongly influenced by the ligand (Figure 4), the amination of n-butyl sulfamate **13** is predicted to be highly γ -selective in reactions with both tpa-

and dmbox-supported Ag nitrenes ($\Delta\Delta G^{\ddagger}$ = 3.9 and 6.8 kcal/ mol, respectively). As the β -C-H bond in 13 is only 1.2 kcal/ mol stronger than the γ -C-H bond, the slopes of the correlations between ΔG^{\ddagger} and C-H BDE in these two types of reactions (0.78 and 0.76 with unactivated C-H bonds in **Types III** and **IV** Ag nitrenes, Figure 5b) predict a moderate γ regioselectivity ($\Delta \Delta G^{\ddagger} \approx 1.0 \text{ kcal/mol}$) as a result of the BDE effects. Clearly, factors other than the BDE difference dominate the γ -selectivity for the reaction with sulfamate 13. The effectiveness of sulfamates in facilitating a sevenmembered ring 1,6-HAT to selectively functionalize γ-C-H bonds²⁵ prompted us to evaluate how the geometrical features of the sulfamate affect the stability of the six-26 and sevenmembered TS in the β - and γ - \dot{C} -H amination pathways, respectively. In C-H insertion transition states with sulfamatederived Ag nitrenes (e.g., TS5- γ and TS5- β , Figure 6), the

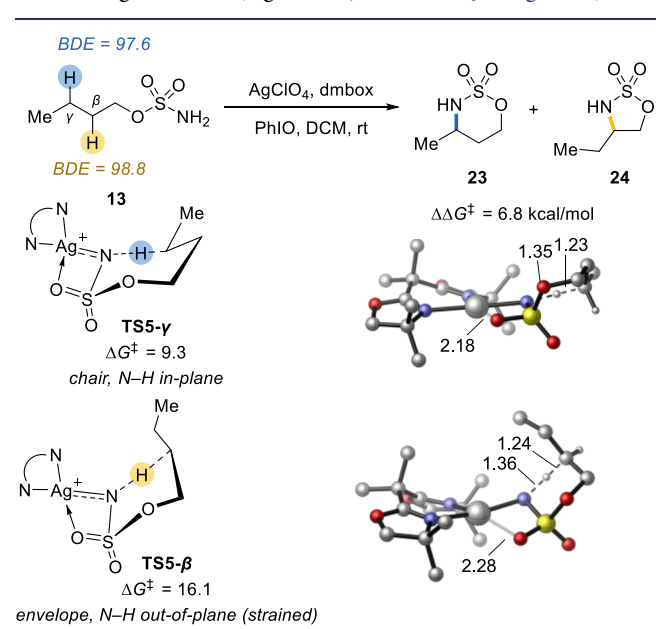


Figure 6. Effects of tether length on the regioselectivity of C-H amination of sulfamate 13 catalyzed by a dmbox-supported Ag catalyst.

seven- and six-membered rings adopt chair-like and envelopelike geometries, respectively. While the chair-like sevenmembered ring in TS5-γ is not strained, substantial strain is present in the envelope-like six-membered ring in TS5- β . In particular, in **TS5-\beta**, the N-H bond in the six-membered ring is not coplanar with the Ag nitrene, furnishing a nonideal angle for the nitrene C-H abstraction. In addition, the envelope conformation in TS5- β leads to greater repulsion with the Ag center because of the concave shape of the bicyclic structure.² The strain of the concave bicyclic system in **TS5-\beta** causes partial dissociation of the sulfonyl coordination to Ag ($d(O\cdots$ Ag) = 2.28 Å, whereas $d(O \cdot \cdot \cdot Ag)$ is 2.18 Å in TS5- γ). In transition states with the carbamate-derived Ag nitrenes (Figure 4), because of the planar geometry of the carbamate group, the seven- and six-membered rings in TS3- γ and TS3- β are nearly coplanar with the Ag catalyst. Thus, the strain in the fused bicyclic system involving carbamate is diminished.

Taken together, the computed transition state structures and energies indicate that high γ -selectivity in the Ag-catalyzed amination of n-butyl sulfamate 13 is due to destabilization of the β -C-H insertion transition state by the ring strain of the

fused bicyclic structure with the six-membered ring. In contrast, ring strain effects are diminished in the amination with n-butyl carbamate 6 because the planar geometry of the carbamate leads to small ring strain in both the β - and γ -C-H insertion transition states.

To investigate whether the different tether length effects between carbamate and sulfamate precursors are applicable to other substrates and to explore whether the ancillary ligand on Ag influences the tether length effect, we computed the C–H insertion activation free energies with various β - and γ -C–H bonds in **Types I–IV** Ag nitrene complexes. These substrates include secondary alkyl C–H bonds and activated C–H bonds, where the C–H BDEs have small effects on their relative reactivities (vide supra, a full list of precursors is available in the Supporting Information, Page S38). For each intramolecular C–H insertion transition state, we also computed a hypothetical, unstrained acyclic C–H insertion transition state (Figure 7). In this manner, we can use the

• TS ring strain energy (ΔH_s) in γ -C–H insertion transition states

LAg X ONe

H 3 X Ethane

ethane

$$AH_s = -\Delta H_{TXIN}$$
 $AH_s = -\Delta H_{TXIN}$
 $AH_s = -\Delta$

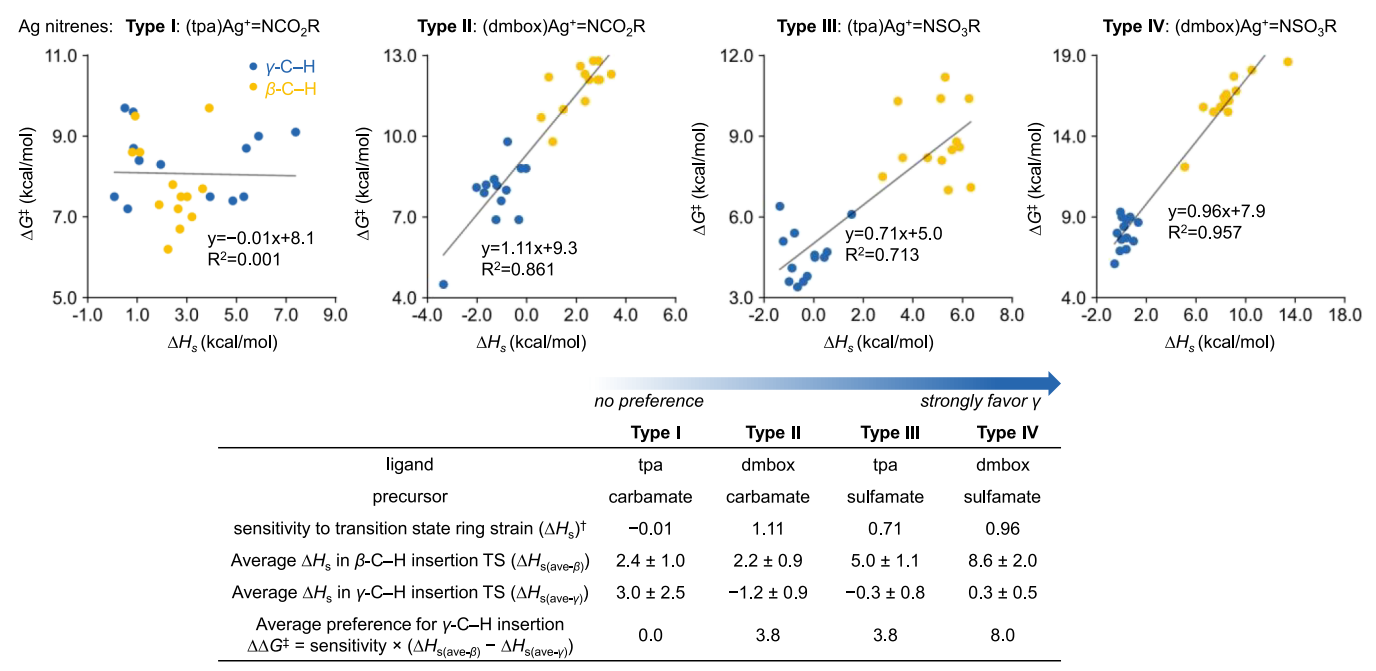
• TS ring strain energy ($\Delta H_{\rm s}$) in β -C–H insertion transition states

LAg
$$X - O$$
 $+ 2 \times O$ ethane $X - O$ $X - O$

Figure 7. Homodesmotic reactions to calculate ring strain energies $(\Delta H_{\rm s})$ of cyclic C–H insertion transition states.

reaction enthalpies of the homodesmotic reactions²⁸ shown in Figure 7 to compute the ring strain energy (ΔH_s) of each cyclic C–H insertion transition state.

The computed activation free energies and transition state ring strain energies (Figure 8) indicate that the γ-C-H insertion is often favored, but the γ -selectivity is significantly affected by both the identity of the precursor and the ancillary ligand on Ag. Among the four types of Ag nitrenes, (dmbox)Ag nitrenes derived from sulfamates (Type IV) have the greatest γ -selectivity—the β -C–H insertion transition states with these complexes suffer from significant ring strain energies $(\Delta H_{\text{s(ave-}\beta)} = 8.6 \pm 2.0 \text{ kcal/mol})$, while the γ -C-H insertion transition states are not strained ($\Delta H_{\text{s(ave-}\gamma)} = 0.3 \pm 0.5 \text{ kcal/}$ mol). In the reactions with tpa-supported sulfamate-derived Ag nitrenes (Type III) and dmbox-supported carbamate-derived Ag nitrenes (**Type II**), the γ -selectivity is lower, due to decreased ring strain in the β -C-H insertion transition states. Finally, the preference for γ -C-H insertion is completely diminished in tpa-supported carbamate-derived Ag nitrenes (**Type I**) because the β - and γ -C-H insertion transition states have comparable ring strain energies. The good correlations between ΔH_s and ΔG^{\ddagger} in the reactions with Types II-IV Ag nitrenes indicate that ring strain in the cyclic transition states plays a significant role in the reactivity and regioselectivity of C-H insertion. Based on the slopes of the correlations



 $^{^{\}dagger}$ Sensitivity is derived from the slope of the correlation between ΔG^{\ddagger} and $\Delta H_{\rm s}$. All energies are in kcal/mol.

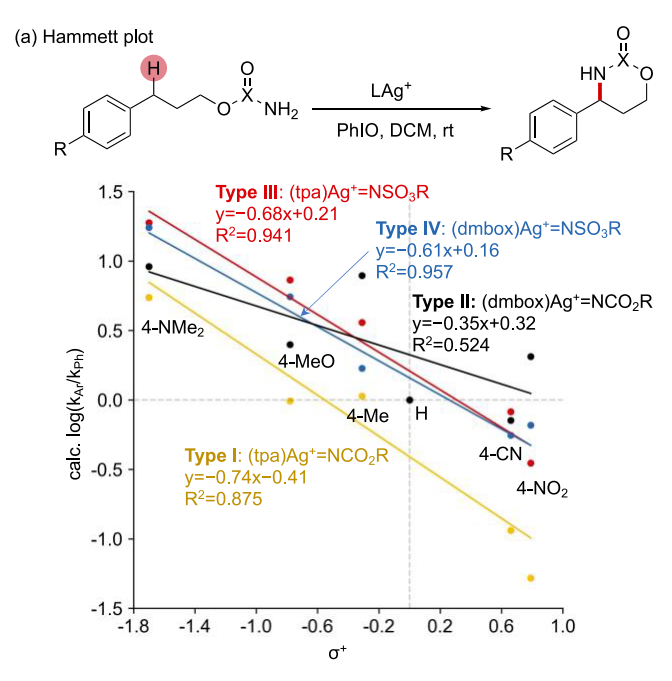
Figure 8. Effects of tether length on transition state ring strain energy (ΔH_s) and activation free energies (ΔG^{\ddagger}) of the β- and γ-C-H insertion with different Ag nitrene complexes.

between ΔH_s and ΔG^{\ddagger} (i.e., sensitivity to ΔH_s) and the average ΔH_s for β - and γ -C-H insertion transition states, we can estimate that the average preference for γ -C-H insertion is 8.0 kcal/mol for Type IV, 3.8 kcal/mol for Types II-III, and 0.0 kcal/mol for Type I Ag nitrenes. This general trend suggests that the magnitude of tether length effects is affected by both the ancillary ligand and the precursor. While Type IV nitrenes have the greatest preference for γ -C-H insertion because of the strain of the concave bicyclic β -C-H insertion TS with this type of Ag nitrene, the β -C-H insertion TS is less strained when the bidentate dmbox ligand is replaced with a multidentate tpa ligand in Type III nitrenes, which weakens the sulfonyl-Ag coordination. For nitrenes containing the planar carbamate group (**Types I and II**), the β -C-H insertion TSs are also less strained because they do not have the concave geometry. The lack of ring strain effects in the reactions with Type I Ag nitrenes makes this type of reaction especially promising for activating β -C-H bonds. These system-dependent tether length effects, combined with other factors that promote selective β -C-H amination, such as ligand-substrate steric repulsions with multidentate ligands (vide supra), 29 provide a general platform for regiodivergent C-H amination for a broad range of substrates.

Electronic Effects of the C–H Bond on Reactivity. The charge transfer from the C–H bond to the Ag nitrene in the C–H insertion transition states (Figure 4b,c) indicates an electrophilic C–H amination mechanism that favors more electron-rich C–H bonds. To evaluate whether the different types of Ag nitrenes have different sensitivities to electronic effects, we computed the activation free energies of a series of benzylic C–H bonds with Types I–IV Ag nitrenes (Figure 9). The four different types of Ag nitrenes all react faster with more electron-rich C–H bonds. Correlations of computed relative rate constants with the σ^+ parameters gave comparable slopes for all four types of nitrenes (Figure 9a). These results indicate that the different Ag nitrenes have a similar

electrophilicity when reacting with the C–H bonds. The computationally derived slope for Type III Ag nitrenes (-0.68) is in good agreement with the experimental Hammett studies with the (tpa)Ag(OTf)-catalyzed intramolecular competition of diaryl sulfamates, which gave a ρ of -0.69 using $\sigma_{\rm p}^{+}$ parameters. Good correlations between the computed activation free energies and NPA charges of the benzylic H atoms (Figure 9b) suggest that the partial atomic charges of the substrates may be used to describe the reactivity preference for more electron-rich C–H bonds in the amination reactions.

Summary of Catalyst-Dependent Factors on Reactivity and Regioselectivity. The computational results discussed above revealed that the regioselectivity of the Agcatalyzed C-H amination is controlled by various factors, including BDE and electronic properties of the C-H bonds, tether length, and ligand-substrate steric repulsions. We summarized the sensitivity to each of these effects for the four different types of Ag nitrenes (Figure 10). Understanding the effects of different substrate parameters on regioselectivity with a given type of Ag nitrene is valuable for the design of regiodivergent C-H aminations. For example, although all four types of Ag nitrenes prefer unactivated C-H bonds with lower BDEs, the lower sensitivity in reactions with tpasupported carbamate-derived Ag nitrenes (Type I) makes them the best catalyst system to pursue the selective functionalization of relatively strong unactivated C-H bonds. By contrast, amination of activated C-H bonds is not sensitive to BDE when carbamate precursors are used (Types I-II). This offers plenty of opportunities to override the BDE preference to aminate, a relatively strong C-H bond in the presence of a weaker activated C-H bond. The strong preference for γ -selectivity using Type IV Ag nitrenes makes the (dmbox)Ag(I)-catalyzed reactions of sulfamates suitable for γ -C-H amination. By contrast, the tpa-supported carbamate-derived Ag nitrenes (Type I) favor amination of



(b) Correlation between activation free energy and NPA charge of the H atom

	NPA charge (H)		
	X = C	X = S=O	
R = NMe ₂	0.214 (25)	0.215 (26)	
MeO	0.216 (27)	0.217 (28)	
Me	0.214 (29)	0.215 (30)	
Н	0.215 (1)	0.216 (22)	
CN	0.220 (31)	0.222 (32)	
NO_2	0.221 (33)	0.222 (34)	

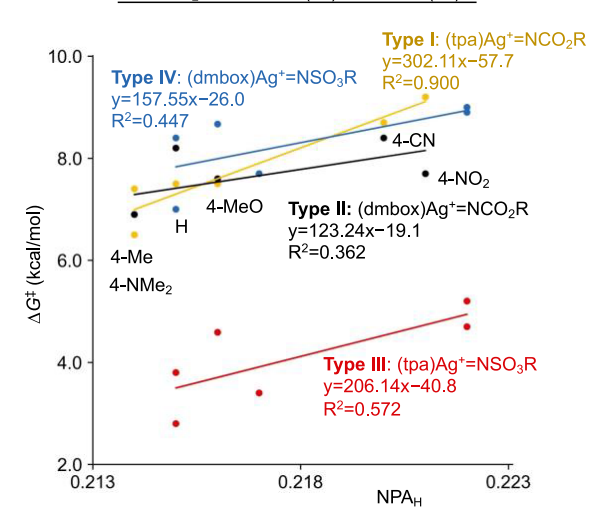


Figure 9. Substrate electronic effects on the reactivity of Ag-catalyzed benzylic C—H aminations.

 β -C-H over γ -C-H bonds, if other factors are equal, due to ligand steric effects. Finally, more electron-rich C-H bonds are preferred, regardless of the ancillary ligand and the nitrene precursor. As discussed above, the different reactivities of the Ag nitrenes are mainly affected by the ligand denticity and whether a sp²-hybridized trigonal planar atom or a sp³-hybridized tetrahedral atom is attached to the nitrene. Therefore, we expect that the same reactivity trends should also apply in Ag-catalyzed C-H amination with other ancillary ligands and precursors.

Experimental Validation of Factors Affecting Regioselectivity. To validate the different selectivity-determining

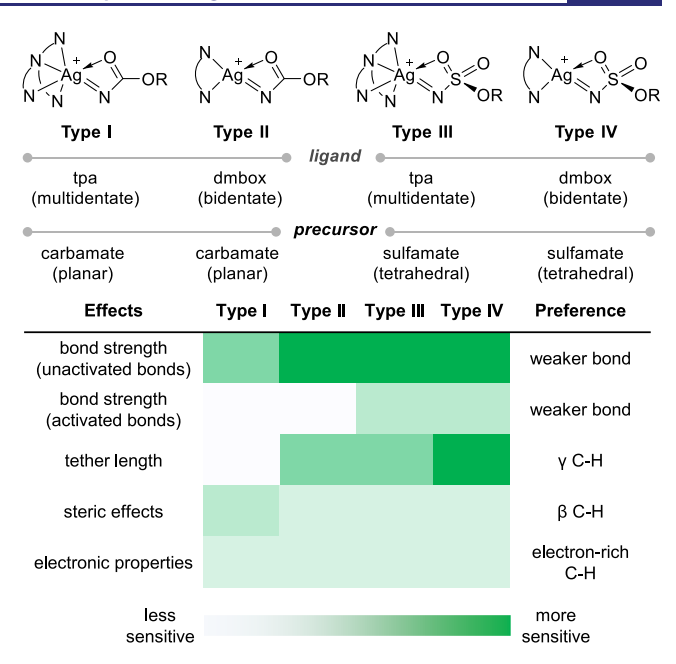


Figure 10. Catalyst-dependent sensitivity of C-H insertion barriers to different substrate properties.

factors summarized in Figure 10, we analyzed the regiose-lectivity of various Ag-catalyzed C–H amination reactions reported in the literature and performed new experiments when the regioselectivity results were not available. We compared the β/γ -selectivity in the amination of *n*-butyl carbamate (6), *n*-butyl sulfamate (13) (Figure 11), and

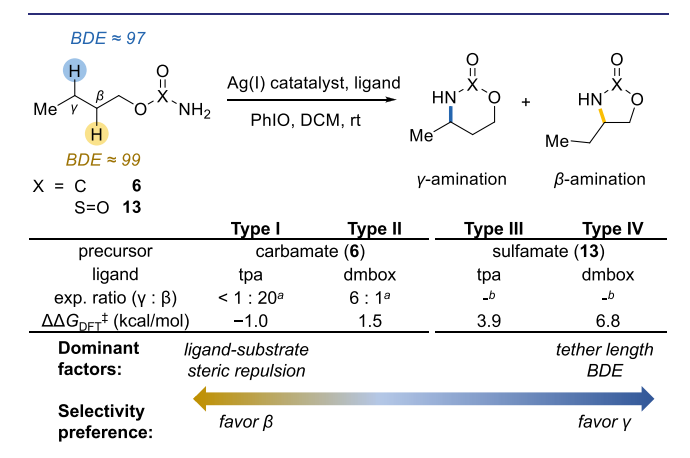


Figure 11. Experimental and computational studies of catalyst-controlled regiodivergent β/γ -selectivity. ^aThis work. ^bThese reactions failed to give the desired C–H amination product due to substrate decomposition or overamination/over-oxidation.

menthol-derived carbamate (35) and sulfamate (36) (Figure 12). In these substrates, the β -C-H bonds have slightly higher BDE than the γ -C-H bonds. According to the factors shown in Figure 10, γ -C-H amination is expected to be strongly preferred in the (dmbox)Ag-catalyzed reactions with sulfamates (Type IV), due to ring strain energy effects, while β -C-H amination should be preferred in the (tpa)Ag-catalyzed reaction with carbamates (Type I) due to ligand-substrate steric repulsions. Indeed, the experimentally observed product ratios agree well with this general selectivity trend and the computationally predicted regioselectivities (Figure 11). The amination of n-butyl carbamate (6) using tpa ligand gave

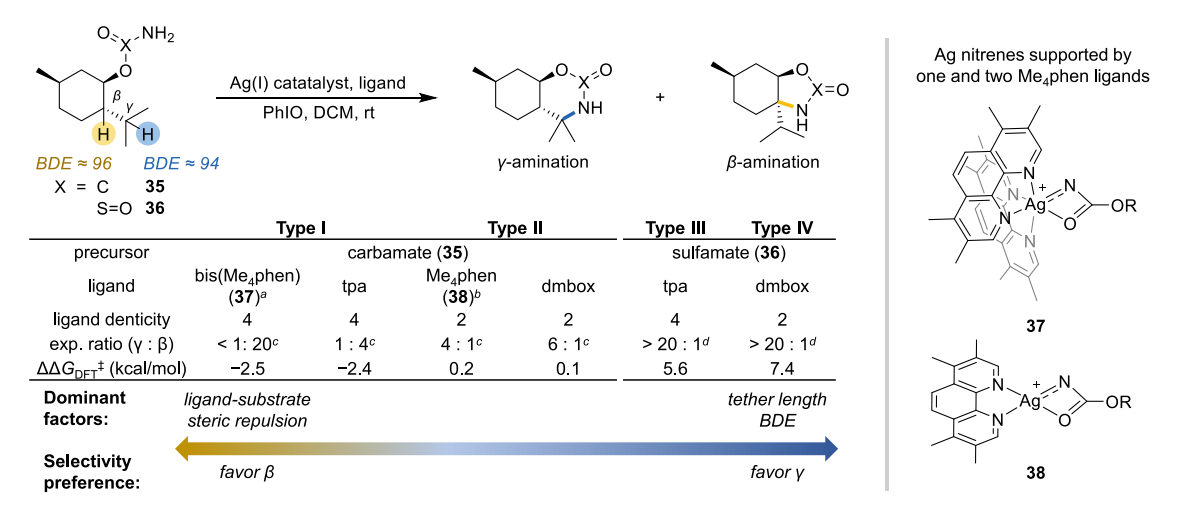


Figure 12. Experimental and computational studies of catalyst-controlled regiodivergent β/γ-selectivity. ^aAg nitrene supported by two Me₄phen ligands (37) was used in the DFT calculations. The experimental regioselectivity was obtained with a 3:1 ratio of Me₄phen:Ag. ^bAg nitrene supported by one Me₄phen ligand (38) was used in the DFT calculations. The experimental regioselectivity was obtained with a 1:1 ratio of Me₄phen:Ag. ^cReported in ref 2b. ^dThis work.

excellent β -selectivity (γ : β < 1: 20). The regioselectivity with the same substrate is completely reversed to favor the γ amination product in a 6:1 ratio when the dmbox ligand is used in place of tpa (see Figures 4 and 6 for computed TS structures and the origin of the catalyst-controlled divergent regioselectivity, respectively). Although reactions using *n*-butyl sulfamate (13) under standard conditions failed to give the desired amination product due to substrate decomposition and side reactions, in the reactions with menthol-derived sulfamate (36), excellent γ -selectivity was obtained (Figure 12). These new experimental results confirmed the strong preference for γ -amination products for **Types III** and **IV** Ag nitrenes. The computational results also agree with the previously reported catalyst-controlled regiodivergent amination of carbamate 35²⁶—when bidentate ligands such as dmbox and Me₄phen are used, the **Type II** Ag nitrenes gave moderate γ -selectivity; in contrast, reactions using multidentate tpa Type I Ag nitrenes favored β -product. The effect of the ligand-to-Ag ratio on the regioselectivity with Me₄phen-supported Ag catalyst is also consistent with this trend—when a 1:1 ratio of Me₄phen:Ag was used, the Type II Ag nitrene supported by the bidentate ligand (38) gave the γ -product; when excess Me₄phen ligand is used, two Me₄phen ligands are expected to bind to the Ag, and thus a Type I Ag nitrene (37) would lead to the preferred β -amination product. These validation experiments supported the strategies discussed above to achieve catalyst-controlled tunable $\beta - / \gamma$ -regioselectivity by altering the ligand denticity and precursor identity.

Next, we compared the computed substrate BDE and electronic effects on reactivity with experimental results. Intramolecular competition experiments have been reported to study the reactivities of benzylic and other activated C–H bonds in the (tpa)Ag(OTf)-catalyzed amination of sulfamates that involve Type III Ag nitrenes (Figure 13). ^{3a,b} These reactions are expected to have small-to-moderate sensitivity to the BDE and electronic properties of the C–H bonds (Figure 10). Both the experimentally observed regioselectivity (Figure 13a,b) and the computationally predicted activation free energies (Supporting Information, tabulated data summary E) support these conclusions. A good agreement between the

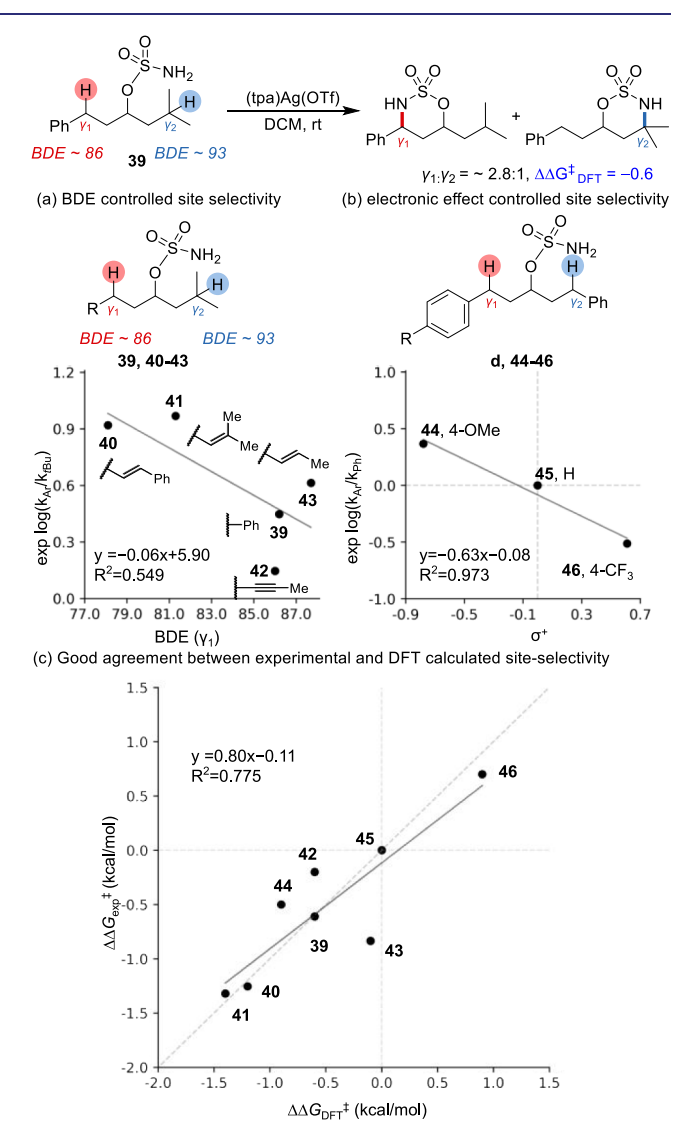


Figure 13. Validation of substrate BDE and electronic effects on regioselectivity.

experimental and DFT-calculated regionselectivity was obtained (Figure 13c).

CONCLUSIONS

A combined computational and experimental study was performed to investigate why different types of Ag nitrene intermediates lead to different regioselectivities in the Agcatalyzed C-H amination. These insights can be used to predict regiodivergent amination of a diverse range of C-H bonds. The computational studies indicated that the Agcatalyzed intramolecular C-H amination reaction proceeds via a concerted H-atom transfer/C-N bond formation process involving singlet Ag nitrene intermediates. The ancillary ligand and the identity of the nitrene precursor (carbamate vs sulfamate) affect the transition state geometry and thus ring strain in the intramolecular C-H insertion and ligandsubstrate steric repulsions. These transition state geometry differences lead to distinct sensitivities of C-H insertion barriers to the different substrate properties, such as tether length, BDE and electronic effects of C-H bonds, and steric repulsions.

The sensitivities to these different effects were investigated for four representative types of Ag nitrenes supported by either a bidentate (i.e., dmbox) or a multidentate (i.e., tpa) ligand and derived from precursors with either a trigonal planar (i.e., carbamate) or a tetrahedral (i.e., sulfamate) atom attached to the nitrene nitrogen. We demonstrated how these reactivity rules can be used to select the best catalyst system to achieve the desired regioselectivity. For example, the Ag-catalyzed aminations with the bidentate dmbox ligand and sulfamate precursors strongly favor γ -C-H bonds. This regioselectivity is reversed by using a tpa-supported Ag catalyst with carbamate precursors. In addition, the (tpa)Ag(OTf)-catalyzed amination of unactivated C-H bonds in carbamate precursors is the least sensitive to the BDE effect. Therefore, this is the most effective catalyst system to promote amination of C-H bonds with stronger BDEs in the presence of weaker BDE C-H bonds.

Overall, this study revealed how the ancillary ligand and precursor affect the stability of the C-H amination transition state and thus can be rationally selected to control the regioselectivity in the Ag-catalyzed C-H aminations. We expect that the interplay of these ring strain, electronic, and steric effects can offer unique insights to guide future design of regiodivergent functionalization strategies and facilitate the catalyst design on challenging C-H amination reactions.

ASSOCIATED CONTENT

Supporting Information

The Supporting Information is available free of charge at https://pubs.acs.org/doi/10.1021/jacs.1c12111.

Additional computational results and experimental details (PDF)

Cartesian coordinates (XYZ)

AUTHOR INFORMATION

Corresponding Authors

Jennifer M. Schomaker — Department of Chemistry, University of Wisconsin, Madison, Wisconsin 53706, United States; orcid.org/0000-0003-1329-950X; Email: schomakerj@chem.wisc.edu

Peng Liu – Department of Chemistry, University of Pittsburgh, Pittsburgh, Pennsylvania 15260, United States; Department

of Chemical and Petroleum Engineering, University of Pittsburgh, Pittsburgh, Pennsylvania 15261, United States; orcid.org/0000-0002-8188-632X; Email: pengliu@pitt.edu

Authors

Yue Fu — Department of Chemistry, University of Pittsburgh, Pittsburgh, Pennsylvania 15260, United States; ⊚ orcid.org/0000-0003-3085-7817

Emily E. Zerull – Department of Chemistry, University of Wisconsin, Madison, Wisconsin 53706, United States

Complete contact information is available at: https://pubs.acs.org/10.1021/jacs.1c12111

Notes

The authors declare no competing financial interest.

ACKNOWLEDGMENTS

We thank the NSF (CHE-1654122 to P.L.; CHE-1954325 to J.M.S.) for financial support for this work. DFT calculations were performed at the Center for Research Computing of the University of Pittsburgh, the TACC Frontera supercomputer, and the Extreme Science and Engineering Discovery Environment (XSEDE) supported by the National Science Foundation grant number ACI-1548562. Y.F. thanks the Andrew W. Mellon Predoctoral Fellowship.

REFERENCES

(1) (a) Müller, P.; Fruit, C. Enantioselective catalytic aziridinations and asymmetric nitrene insertions into C-H bonds. Chem. Rev. 2003, 103, 2905-2920. (b) Díaz-Requejo, M. M.; Belderraín, T. R.; Nicasio, M. C.; Trofimenko, S.; Pérez, P. J. Cyclohexane and Benzene Amination by Catalytic Nitrene Insertion into C-H Bonds with the Copper-Homoscorpionate Catalyst TpBr3Cu(NCMe). J. Am. Chem. Soc. 2003, 125, 12078-12079. (c) Li, Z.; Capretto, D. A.; Rahaman, R.; He, C. Silver-Catalyzed Intermolecular Amination of C-H Groups. Angew. Chem., Int. Ed. 2007, 46, 5184-5186. (d) Roizen, J. L.; Harvey, M. E.; Du Bois, J. Metal-Catalyzed Nitrogen-Atom Transfer Methods for the Oxidation of Aliphatic C-H Bonds. Acc. Chem. Res. 2012, 45, 911-922. (e) Hazelard, D.; Nocquet, P. A.; Compain, P. Catalytic C-H amination at its limits: challenges and solutions. Org. Chem. Front. 2017, 4, 2500-2521. (f) Park, Y.; Kim, Y.; Chang, S. Transition Metal-Catalyzed C-H Amination: Scope, Mechanism, and Applications. Chem. Rev. 2017, 117, 9247-9301. (g) Lang, K.; Torker, S.; Wojtas, L.; Zhang, X. P. Asymmetric Induction and Enantiodivergence in Catalytic Radical C-H Amination via Enantiodifferentiative H-Atom Abstraction and Stereoretentive Radical Substitution. J. Am. Chem. Soc. 2019, 141, 12388-12396. (h) Lang, K.; Li, C.; Kim, I.; Zhang, X. P. Enantioconvergent Amination of Racemic Tertiary C-H Bonds. J. Am. Chem. Soc. 2020, 142, 20902-20911.

(2) (a) Alderson, J. M.; Corbin, J. R.; Schomaker, J. M. Tunable, Chemo- and Site-Selective Nitrene Transfer Reactions through the Rational Design of Silver(I) Catalysts. *Acc. Chem. Res.* **2017**, *50*, 2147–2158. (b) Ju, M.; Huang, M.; Vine, L. E.; Dehghany, M.; Roberts, J. M.; Schomaker, J. M. Tunable Catalyst-Controlled Syntheses of β - and γ -Amino Alcohols Enabled by Silver-Catalysed Nitrene Transfer. *Nat. Catal.* **2019**, *2*, 899–908. (c) Vine, L. E.; Zerull, E. E.; Schomaker, J. M. Taming Nitrene Reactivity with Silver Catalysts. *Synlett* **2021**, *32*, 30–44.

(3) (a) Alderson, J. M.; Phelps, A. M.; Scamp, R. J.; Dolan, N. S.; Schomaker, J. M. Ligand-Controlled, Tunable Silver-Catalyzed C-H Amination. *J. Am. Chem. Soc.* **2014**, *136*, 16720–16723. (b) Huang, M.; Yang, T.; Paretsky, J. D.; Berry, J. F.; Schomaker, J. M. Inverting Steric Effects: Using "Attractive" Noncovalent Interactions to Direct Silver-Catalyzed Nitrene Transfer. *J. Am. Chem. Soc.* **2017**, *139*,

- 17376–17386. (c) Alderson, J. M.; Corbin, J. R.; Schomaker, J. M. Investigation of Transition Metal-Catalyzed Nitrene Transfer Reactions in Water. *Bioorg. Med. Chem.* **2018**, *26*, 5270–5273. (d) Huh, S.; Hong, S. Y.; Chang, S. Synthetic Utility of N-Benzoyloxyamides as an Alternative Precursor of Acylnitrenoids for γ -Lactam Formation. *Org. Lett.* **2019**, *21*, 2808–2812. (e) Jung, H.; Keum, H.; Kweon, J.; Chang, S. Tuning Triplet Energy Transfer of Hydroxamates as the Nitrene Precursor for Intramolecular C(Sp3)–H Amidation. *J. Am. Chem. Soc.* **2020**, *142*, 5811–5818.
- (4) Frisch, M. J.; Trucks, G. W.; Schlegel, H. B.; Scuseria, G. E.; Robb, M. A.; Cheeseman, J. R.; Scalmani, G.; Barone, V.; Petersson, G. A.; Nakatsuji, H.; Li, X.; Caricato, M.; Marenich, A. V.; Bloino, J.; Janesko, B. G.; Gomperts, R.; Mennucci, B.; Hratchian, H. P.; Ortiz, J. V.; Izmaylov, A. F.; Sonnenberg, J. L.; Ding, F.; Lipparini, F.; Egidi, F.; Goings, J.; Peng, B.; Petrone, A.; Henderson, T.; Ranasinghe, D.; Zakrzewski, V. G.; Gao, J.; Rega, N.; Zheng, G.; Liang, W.; Hada, M.; Ehara, M.; Toyota, K.; Fukuda, R.; Hasegawa, J.; Ishida, M.; Nakajima, T.; Honda, Y.; Kitao, O.; Nakai, H.; Vreven, T.; Throssell, K.; Montgomery, Jr., J. A.; Peralta, J. E.; Ogliaro, F.; Bearpark, M. J.; Heyd, J. J.; Brothers, E. N.; Kudin, K. N.; Staroverov, V. N.; Keith, T. A.; Kobayashi, R.; Normand, J.; Raghavachari, K.; Rendell, A. P.; Burant, J. C.; Iyengar, S. S.; Tomasi, J.; Cossi, M.; Millam, J. M.; Klene, M.; Adamo, C.; Cammi, R.; Ochterski, J. W.; Martin, R. L.; Morokuma, K.; Farkas, O.; Foresman, J. B.; Fox, D. J. Gaussian 16 Rev. B.01; Gaussian, Inc.: Wallingford, CT, 2016.
- (5) Chai, J.-D.; Head-Gordon, M. Long-Range Corrected Hybrid Density Functionals with Damped Atom—Atom Dispersion Corrections. *Phys. Chem. Chem. Phys.* **2008**, *10*, 6615–6620.
- (6) Marenich, A. V.; Cramer, C. J.; Truhlar, D. G. Universal Solvation Model Based on Solute Electron Density and on a Continuum Model of the Solvent Defined by the Bulk Dielectric Constant and Atomic Surface Tensions. *J. Phys. Chem. B* **2009**, *113*, 6378–6396.
- (7) Pracht, P.; Bohle, F.; Grimme, S. Automated Exploration of the Low-Energy Chemical Space with Fast Quantum Chemical Methods. *Phys. Chem. Chem. Phys.* **2020**, *22*, 7169–7192.
- (8) Bannwarth, C.; Ehlert, S.; Grimme, S. GFN2-XTB—An Accurate and Broadly Parametrized Self-Consistent Tight-Binding Quantum Chemical Method with Multipole Electrostatics and Density-Dependent Dispersion Contributions. *J. Chem. Theory Comput.* **2019**, *15*, 1652–1671.
- (9) Luchini, G.; Alegre-Requena, J. V.; Funes-Ardoiz, I.; Paton, R. S. GoodVibes: automated thermochemistry for heterogeneous computational chemistry data. *F1000 Research* **2020**, *9*, 291.
- (10) (a) Werner, H.-J.; Knowles, P. J.; Knizia, G.; Manby, F. R.; Schütz, M. Molpro: A General-Purpose Quantum Chemistry Program Package. WIREs Comput. Mol. Sci. 2012, 2, 242—253. (b) Werner, H.-J.; Knowles, P. J.; Manby, F. R.; Black, J. A.; Doll, K.; Heßelmann, A.; Kats, D.; Köhn, A.; Korona, T.; Kreplin, D. A.; Ma, Q.; Miller, T. F.; Mitrushchenkov, A.; Peterson, K. A.; Polyak, I.; Rauhut, G.; Sibaev, M. The Molpro Quantum Chemistry Package. J. Chem. Phys. 2020, 152, 144107.
- (11) Ma, Q.; Werner, H. J. Scalable Electron Correlation Methods. 8. Explicitly Correlated Open-Shell Coupled-Cluster with Pair Natural Orbitals PNO-RCCSD(T)-F12 and PNO-UCCSD(T)-F12. *J. Chem. Theory Comput.* **2021**, *17*, 902–926.
- (12) Ma, Q.; Werner, H.-J. Accurate Intermolecular Interaction Energies Using Explicitly Correlated Local Coupled Cluster Methods [PNO-LCCSD(T)-F12]. J. Chem. Theory Comput. 2019, 15, 1044–1052.
- (13) (a) Fdez, G. I.; Vacher, M.; Alavi, A.; Angeli, C.; Aquilante, F.; Autschbach, J.; Bao, J. J.; Bokarev, S. I.; Bogdanov, N. A.; Carlson, R. K.; Chibotaru, L. F.; Creutzberg, J.; Dattani, N.; Delcey, M. G.; Dong, S. S.; Dreuw, A.; Freitag, L.; Frutos, L. M.; Gagliardi, L.; Gendron, F.; Giussani, A.; González, L.; Grell, G.; Guo, M.; Hoyer, C. E.; Johansson, M.; Keller, S.; Knecht, S.; Kovačević, G.; Källman, E.; Li Manni, G.; Lundberg, M.; Ma, Y.; Mai, S.; Malhado, J. P.; Malmqvist, P. Å.; Marquetand, P.; Mewes, S. A.; Norell, J.; Olivucci, M.; Oppel, M.; Phung, Q. M.; Pierloot, K.; Plasser, F.; Reiher, M.; Sand, A. M.;

- Schapiro, I.; Sharma, P.; Stein, C. J.; Sørensen, L. K.; Truhlar, D. G.; Ugandi, M.; Ungur, L.; Valentini, A.; Vancoillie, S.; Veryazov, V.; Weser, O.; Wesołowski, T. A.; Widmark, P.-O.; Wouters, S.; Zech, A.; Zobel, J. P.; Lindh, R. OpenMolcas: From Source Code to Insight. J. Chem. Theory Comput. 2019, 15, 5925–5964. (b) Aquilante, F.; Autschbach, J.; Baiardi, A.; Battaglia, S.; Borin, V. A.; Chibotaru, L. F.; Conti, I.; De Vico, L.; Delcey, M.; Galván, I.; Ferré, N.; Freitag, L.; Garavelli, M.; Gong, X.; Knecht, S.; Larsson, E. D.; Lindh, R.; Lundberg, M.; Malmqvist, P. Å.; Nenov, A.; Norell, J.; Odelius, M.; Olivucci, M.; Pedersen, T. B.; Pedraza-González, L.; Phung, Q. M.; Pierloot, K.; Reiher, M.; Schapiro, I.; Segarra-Martí, J.; Segatta, F.; Seijo, L.; Sen, S.; Sergentu, D.-C.; Stein, C. J.; Ungur, L.; Vacher, M.; Valentini, A.; Veryazov, V. Modern Quantum Chemistry with [Open] Molcas. J. Chem. Phys. 2020, 152, 214117.
- (14) Coupled cluster and CASPT2 methods are frequently used to access the accuracy of DFT calculations. See (a) Matsui, J. K.; Gutiérrez-Bonet, Á.; Rotella, M.; Alam, R.; Gutierrez, O.; Molander, G. A. Photoredox/Nickel-Catalyzed Single-Electron Tsuji-Trost Reaction: Development and Mechanistic Insights. Angew. Chem., Int. Ed. 2018, 57, 15847-15851. (b) Radoń, M. Benchmarking Quantum Chemistry Methods for Spin-State Energetics of Iron Complexes against Quantitative Experimental Data. Phys. Chem. Chem. Phys. 2019, 21, 4854-4870. (c) Yang, Y.; Cho, I.; Qi, X.; Liu, P.; Arnold, F. H. An Enzymatic Platform for the Asymmetric Amination of Primary, Secondary and Tertiary C(Sp 3)-H Bonds. Nat. Chem. 2019, 11, 987-993. (d) Yuan, M.; Song, Z.; Badir, S. O.; Molander, G. A.; Gutierrez, O. On the Nature of C(Sp3)-C(Sp2) Bond Formation in Nickel-Catalyzed Tertiary Radical Cross-Couplings: A Case Study of Ni/Photoredox Catalytic Cross-Coupling of Alkyl Radicals and Aryl Halides. J. Am. Chem. Soc. 2020, 142, 7225-7234. (e) Lin, Q.; Fu, Y.; Liu, P.; Diao, T. Monovalent Nickel-Mediated Radical Formation: A Concerted Halogen-Atom Dissociation Pathway Determined by Electroanalytical Studies. J. Am. Chem. Soc. 2021, 143, 14196-14206. (f) Nair, V. N.; Kojasoy, V.; Laconsay, C. J.; Kong, W. Y.; Tantillo, D. J.; Tambar, U. K. Catalyst-Controlled Regiodivergence in Rearrangements of Indole-Based Onium Ylides. J. Am. Chem. Soc. 2021, 143, 9016-9025.
- (15) (a) Gómez-Emeterio, B. P.; Urbano, J.; Díaz-Requejo, M. M.; Pérez, P. J. Easy Alkane Catalytic Functionalization. *Organometallics* **2008**, 27, 4126–4130. (b) Collet, F.; Lescot, C.; Dauban, P. Catalytic C–H Amination: The Stereoselectivity Issue. *Chem. Soc. Rev.* **2011**, 40, 1926–1936.
- (16) For κ²-coordinated Cu nitrene complexes, see (a) Moegling, J.; Hoffmann, A.; Thomas, F.; Orth, N.; Liebhäuser, P.; Herber, U.; Rampmaier, R.; Stanek, J.; Fink, G.; Ivanović-Burmazović, I.; Herres-Pawlis, S.; et al. *Angew. Chem., Int. Ed.* **2018**, *57*, 9154–9159. (b) Thomas, F.; Oster, M.; Schön, F.; Göbgen, K. C.; Amarouch, B.; Steden, D.; Hoffmann, A.; Herres-Pawlis, S. A New Generation of Terminal Copper Nitrenes and Their Application in Aromatic C–H Amination Reactions. *Dalton Trans.* **2021**, *50*, 6444–6462.
- (17) Because PhIO is insoluble, mass-transport may also be the rate-determining step. Previously reported nonideal kinetic behavior suggested that the solubility of PhIO may affect the reaction rate. See Weatherly, C.; Alderson, J. M.; Berry, J. F.; Hein, J. E.; Schomaker, J. M. Catalyst-Controlled Nitrene Transfer by Tuning Metal:Ligand Ratios: Insight into the Mechanisms of Chemoselectivity. *Organometallics* 2017, 36, 1649–1661.
- (18) To the best of our knowledge, Ag nitrene intermediates in Ag NT reactions have not been isolated. For characterization of Rh nitrene complexes, see (a) Das, A.; Chen, Y.-S.; Reibenspies, J. H.; Powers, D. C. Characterization of a Reactive Rh2 Nitrenoid by Crystalline Matrix Isolation. *J. Am. Chem. Soc.* **2019**, *141*, 16232–16236. (b) Das, A.; Wang, C.-H.; Van Trieste, G. P.; Sun, C.-J.; Chen, Y.-S.; Reibenspies, J. H.; Powers, D. C. In Crystallo Snapshots of Rh2-Catalyzed C—H Amination. *J. Am. Chem. Soc.* **2020**, *142*, 19862–19867.
- (19) (a) Maestre, L.; Sameera, W. M. C.; Díaz-Requejo, M. M.; Maseras, F.; Pérez, P. J. A General Mechanism for the Copper- and Silver-Catalyzed Olefin Aziridination Reactions: Concomitant In-

- volvement of the Singlet and Triplet Pathways. *J. Am. Chem. Soc.* **2013**, *135*, 1338–1348. (b) Dolan, N. S.; Scamp, R. J.; Yang, T.; Berry, J. F.; Schomaker, J. M. Catalyst-Controlled and Tunable, Chemoselective Silver-Catalyzed Intermolecular Nitrene Transfer: Experimental and Computational Studies. *J. Am. Chem. Soc.* **2016**, *138*, 14658–14667.
- (20) Short, M. A.; Blackburn, J. M.; Roizen, J. L. Modifying Positional Selectivity in C–H Functionalization Reactions with Nitrogen-Centered Radicals: Generalizable Approaches to 1,6-Hydrogen-Atom Transfer Processes. *Synlett* **2020**, *31*, 102–116.
- (21) (a) Chen, M. S.; White, M. C. A Predictably Selective Aliphatic C–H Oxidation Reaction for Complex Molecule Synthesis. *Science* **2007**, *318*, 783–787. (b) Christina, W. M. Combined Effects on Selectivity in Fe-Catalyzed Methylene Oxidation. *Science* **2010**, *327*, 566–571.
- (22) Badiei, Y. M.; Dinescu, A.; Dai, X.; Palomino, R. M.; Heinemann, F. W.; Cundari, T. R.; Warren, T. H. Copper—Nitrene Complexes in Catalytic C—H Amination. *Angew. Chem., Int. Ed.* **2008**, 47, 9961—9964.
- (23) For bimodal relationships between C-H BDE and the reactivity of dioxirane-mediated C-H oxidations, see Liu, F.; Yang, Z.; Yu, Y.; Mei, Y.; Houk, K. N. Bimodal Evans-Polanyi Relationships in Dioxirane Oxidations of Sp3 C-H: Non-Perfect Synchronization in Generation of Delocalized Radical Intermediates. *J. Am. Chem. Soc.* 2017, 139, 16650–16656.
- (24) Salamone, M.; Galeotti, M.; Romero-Montalvo, E.; van Santen, J. A.; Groff, B. D.; Mayer, J. M.; DiLabio, G. A.; Bietti, M. Bimodal Evans—Polanyi Relationships in Hydrogen Atom Transfer from C(Sp3)—H Bonds to the Cumyloxyl Radical. A Combined Time-Resolved Kinetic and Computational Study. *J. Am. Chem. Soc.* **2021**, 143, 11759—11776.
- (25) (a) Espino, C. G.; Fiori, K. W.; Kim, M.; Du Bois, J. Expanding the Scope of C-H Amination through Catalyst Design. J. Am. Chem. Soc. 2004, 126, 15378-15379. (b) Kurokawa, T.; Kim, M.; Du Bois, J. Synthesis of 1,3-Diamines Through Rhodium-Catalyzed C-H Insertion. Angew. Chem., Int. Ed. 2009, 48, 2777-2779. (c) Lu, H.; Jiang, H.; Wojtas, L.; Zhang, X. P. Selective Intramolecular C-H Amination through the Metalloradical Activation of Azides: Synthesis of 1,3-Diamines under Neutral and Nonoxidative Conditions. Angew. Chem., Int. Ed. 2010, 49, 10192-10196. (d) Lu, H.; Hu, Y.; Jiang, H.; Wojtas, L.; Zhang, X. P. Stereoselective Radical Amination of Electron-Deficient C(Sp3)-H Bonds by Co(II)-Based Metalloradical Catalysis: Direct Synthesis of α -Amino Acid Derivatives via α -C-H Amination. Org. Lett. 2012, 14, 5158-5161. (e) Duhamel, T.; Martínez, M. D.; Sideri, I. K.; Muñiz, K. 1,3-Diamine Formation from an Interrupted Hofmann-Löffler Reaction: Iodine Catalyst Turnover through Ritter-Type Amination. ACS Catal. 2019, 9, 7741-7745. (f) Short, M. A.; Shehata, M. F.; Sanders, M. A.; Roizen, J. L. Sulfamides Direct Radical-Mediated Chlorination of Aliphatic C-H Bonds. Chem. Sci. 2020, 11, 217-223.
- (26) Lu, H.; Lang, K.; Jiang, H.; Wojtas, L.; Zhang, X. P. Intramolecular 1,5-C(Sp3)—H Radical Amination via Co(Ii)-Based Metalloradical Catalysis for Five-Membered Cyclic Sulfamides. *Chem. Sci.* **2016**, *7*, 6934–6939.
- (27) Vorberg, R.; Trapp, N.; Carreira, E. M.; Müller, K. Bicyclo[3.2.0]Heptane as a Core Structure for Conformational Locking of 1,3-Bis-Pharmacophores, Exemplified by GABA. *Chem. Eur. J.* **2017**, 23, 3126–3138.
- (28) (a) Wheeler, S. E.; Houk, K. N.; Schleyer, P. V. R.; Allen, W. D. A Hierarchy of Homodesmotic Reactions for Thermochemistry. *J. Am. Chem. Soc.* **2009**, *131*, 2547–2560. (b) Bach, R. D. Ring Strain Energy in the Cyclooctyl System. The Effect of Strain Energy on [3 + 2] Cycloaddition Reactions with Azides. *J. Am. Chem. Soc.* **2009**, *131*, 5233–5243. (c) Zhang, X.; Lu, G.; Sun, M.; Mahankali, M.; Ma, Y.; Zhang, M.; Hua, W.; Hu, Y.; Wang, Q.; Chen, J.; He, G.; Qi, X.; Shen, W.; Liu, P.; Chen, G. A General Strategy for Synthesis of Cyclophane-Braced Peptide Macrocycles via Palladium-Catalysed Intramolecular Sp3 C–H Arylation. *Nat. Chem.* **2018**, *10*, 540–548.

- (29) Another factor that may impact the catalyst-controlled regioselectivity is whether a mononuclear or dinuclear Ag nitrene is involved in the C–H amination. For example, He et al. reported β -selective amination of carbamates catalyzed by a dinuclear Ag catalyst (ref 1c). The more crowded steric environment of the dimeric Ag catalyst may contribute to the β -selectivity due to steric effects similar to mononuclear Ag catalysts supported by multidentate ligands.
- (30) Ess, D. H.; Nielsen, R. J.; Goddard, W. A., III; Periana, R. A. Transition-State Charge Transfer Reveals Electrophilic, Ambiphilic, and Nucleophilic Carbon—Hydrogen Bond Activation. *J. Am. Chem. Soc.* **2009**, *131*, 11686—11688.
- (31) For Hammett studies of C-H amination via nitrene transfer catalyzed by other transition metal catalysts, see (a) Fiori, K. W.; Espino, C. G.; Brodsky, B. H.; Du Bois, J. A Mechanistic Analysis of the Rh-Catalyzed Intramolecular C-H Amination Reaction. *Tetrahedron* 2009, 65, 3042–3051. (b) Bagchi, V.; Paraskevopoulou, P.; Das, P.; Chi, L.; Wang, Q.; Choudhury, A.; Mathieson, J. S.; Cronin, L.; Pardue, D. B.; Cundari, T. R.; Mitrikas, G.; Sanakis, Y.; Stavropoulos, P. A Versatile Tripodal Cu(I) Reagent for C-N Bond Construction via Nitrene-Transfer Chemistry: Catalytic Perspectives and Mechanistic Insights on C-H Aminations/Amidinations and Olefin Aziridinations. *J. Am. Chem. Soc.* 2014, 136, 11362–11381.